

Boosted dibosons from mixed heavy top squarks

Diptimoy Ghosh*

INFN, Sezione di Roma, Piazzale A. Moro 2, I-00185 Roma, Italy and Fermilab, P.O. Box 500, Batavia, Illinois 60510, USA

(Received 14 August 2013; published 19 December 2013)

The lighter mass eigenstate (\tilde{t}_1) of the two top squarks, the scalar superpartners of the top quark, is extremely difficult to discover if it is almost degenerate with the lightest neutralino ($\tilde{\chi}_1^0$), the lightest stable supersymmetric particle in the R-parity conserving supersymmetry. The current experimental bound on \tilde{t}_1 mass in this scenario stands only around 200 GeV. For such a light \tilde{t}_1 , the heavier top squark (\tilde{t}_2) can also be around the TeV scale. Moreover, the high value of the Higgs (h) mass prefers the left- and right-handed top squarks to be highly mixed, allowing the possibility of a considerable branching ratio for $\tilde{t}_2 \rightarrow \tilde{t}_1 h$ and $\tilde{t}_2 \rightarrow \tilde{t}_1 Z$. In this paper, we explore the above possibility together with the pair production of $\tilde{t}_2 \tilde{t}_2^*$, giving rise to the spectacular diboson + missing transverse energy final state. For an approximately 1 TeV \tilde{t}_2 and a few hundred GeV \tilde{t}_1 the final state particles can be moderately boosted, which encourages us to propose a novel search strategy employing the jet substructure technique to tag the boosted h and Z . The reconstruction of the h and Z momenta also allows us to construct the transverse mass M_{T2} , providing an additional efficient handle to fight the backgrounds. We show that a 4–5 σ signal can be observed at the 14 TeV LHC for ~ 1 TeV \tilde{t}_2 with 100 fb $^{-1}$ integrated luminosity.

DOI: [10.1103/PhysRevD.88.115013](https://doi.org/10.1103/PhysRevD.88.115013)

PACS numbers: 14.80.Da, 12.60.Jv, 13.85.Rm, 14.80.Ly

I. INTRODUCTION

A light third generation of superpartners remains an attractive possibility to realize weak scale supersymmetry (SUSY) [1] in nature even after the successful completion of the 8 TeV run of the Large Hadron Collider (LHC). Moreover, if a light top squark \tilde{t}_1 is the next-to-lightest SUSY particle (NLSP) just above the lightest neutralino ($\tilde{\chi}_1^0$), the lightest stable SUSY particle (LSP) in the R-parity conserving version of the minimally supersymmetric Standard Model (MSSM), it would have a significant density to coexist with the LSP around the freeze-out time, and annihilations involving \tilde{t}_1 with the LSP [2] can help achieve the LSP relic density consistent with the upper bound $\Omega^{\text{DM}} h^2 < 0.128(3\sigma)$ presented by the Planck Collaboration [3].

Such a light \tilde{t}_1 with a very small mass difference with the LSP ($\Delta m \equiv m_{\tilde{t}_1} - m_{\tilde{\chi}_1^0} \lesssim 50$ GeV) will dominantly decay to a charm quark and the LSP [4,5], resulting in a final state with jets and missing transverse momentum (\cancel{p}_T). Owing to the small Δm , both the charm jet and the \cancel{p}_T will be extremely soft on average, making this scenario very challenging to discover experimentally [6–11].

The ATLAS Collaboration has recently excluded a \tilde{t}_1 mass of 200 GeV (95% C.L.) in this channel for $\Delta m < 85$ GeV, using 20.3 fb $^{-1}$ of data collected at the 8 TeV run of the LHC [12]. This result clearly shows the low sensitivity of the current experimental searches to probe the degenerate top squark NLSP region. Hence, it is extremely important to consider other possible signatures of light third generation SUSY in the top squark NLSP scenario.

Interestingly, in this region of the SUSY parameter space, the heavier top squark \tilde{t}_2 can also be below or around the TeV scale, and it could prove useful to also look for them at the LHC. Motivated by this, we, in this paper, propose a novel search strategy to look for signatures of \tilde{t}_2 at the 14 TeV run of the LHC. Note that the signatures of \tilde{t}_2 production at the LHC have not received enough attention in the literature in the recent past, primarily because of the comparatively lower cross section (due to its heaviness).¹ However, with a few hundred fb $^{-1}$ integrated luminosity expected at the 14 TeV LHC, the \tilde{t}_2 production processes could be promising and can even provide information complementary to the \tilde{t}_1 production channels.

In this paper, we consider the pair production of $\tilde{t}_2 \tilde{t}_2^*$ and their subsequent decay to either $\tilde{t}_1 Z$ or $\tilde{t}_1 h$ final states (see Fig. 1). Note that, for the two above decays to have considerable branching ratios, it is necessary to have adequate left-right mixing in the top squark mass matrix [14,15]. Interestingly, the large radiative corrections to the Higgs mass required for the consistency with the experimental observation also prefer the left- and right-handed top squarks to be highly mixed. Hence, the two decay modes $\tilde{t}_2 \rightarrow \tilde{t}_1 Z$ and $\tilde{t}_2 \rightarrow \tilde{t}_1 h$ are indeed very well motivated, in particular in the context of the Higgs discovery. In addition, if most of the electroweak gauginos except the LSP and the sbottoms are rather heavy, which can indeed happen in a large region of the SUSY parameter space, the branching ratio of \tilde{t}_2 to $\tilde{t}_1 Z$ or $\tilde{t}_1 h$ can be significant.

¹See, however, [13] where the authors considered a very low \tilde{t}_2 mass which in turn forced them to assume new F-term or D-term contributions to the Higgs mass beyond the MSSM.

*diptimoy.ghosh@roma1.infn.it

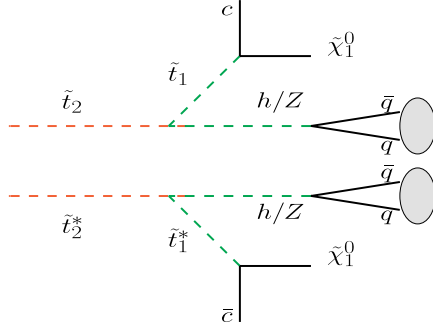


FIG. 1 (color online). Diagram showing a diboson final state originating from $\tilde{t}_2 \tilde{t}_2^*$ pair production.

As we consider the top squark NLSP scenario with a very small Δm , the \tilde{t}_1 dominantly decays via $\tilde{t}_1 \rightarrow c \tilde{\chi}_1^0$. This gives rise to a final state consisting of $hh/hZ/ZZ + \cancel{p}_T$ + very soft jets. Moreover, for an approximately TeV scale \tilde{t}_2 , the decay products are sufficiently boosted and hence, a boosted diboson system (h or Z) along with moderately large \cancel{p}_T is the experimental signature of such a scenario.

In the next section, we will choose a couple of benchmark models where the specific decay chain mentioned above can be realized. The details of our event selection procedure will be discussed in Sec. III. In Sec. IV we will present the final results for our signal as well as the backgrounds and conclude thereafter with some remarks.

II. SUSY MASS SPECTRUM

We now briefly discuss the MSSM mass spectrum relevant for our study and present a couple a benchmark models that will be used to present our results in Sec. IV. In Fig. 2 we graphically show the spectrum for one of our benchmark models (model 1) where the two conditions,

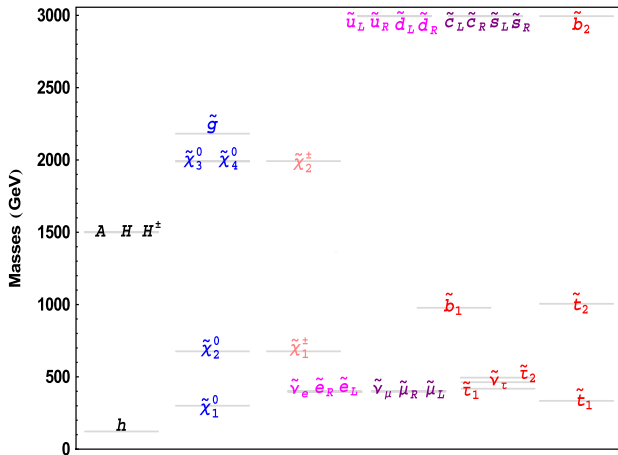


FIG. 2 (color online). Mass spectrum of the MSSM particles for our benchmark model 1.

TABLE I. The relevant pMSSM input parameters, particle masses, and branching ratios for our two benchmark models. The mass spectrum and the branching ratios are calculated using the public package SUSY-HIT [16].

Model 1		Model 2	
pMSSM inputs	Masses	pMSSM inputs	Masses
$M_1 = 300$	$m_{\tilde{t}_2} = 1005$	$M_1 = 410$	$m_{\tilde{t}_2} = 1003$
$M_2 = 650$	$m_{\tilde{t}_1} = 334$	$M_2 = 850$	$m_{\tilde{t}_1} = 434$
$M_3 = 2100$	$m_{\tilde{\chi}_1^0} = 300$	$M_3 = 2600$	$m_{\tilde{\chi}_1^0} = 411$
$\mu = 2000$	$m_{\tilde{\chi}_2^0} = 676$	$\mu = 2000$	$m_{\tilde{\chi}_2^0} = 884$
$m_A = 1500$	$m_{\tilde{\chi}_1^\pm} = 676$	$m_A = 1500$	$m_{\tilde{\chi}_1^\pm} = 884$
$\tan \beta = 10$	$m_h = 123$	$\tan \beta = 7.5$	$m_h = 123$
$m_{Q3} = 1010$		$m_{Q3} = 1050$	
$m_{tR} = 630$		$m_{tR} = 770$	
$m_{bR} = 3000$		$m_{bR} = 3000$	
$A_t = -1700$		$A_t = -1600$	
	$\mathcal{B}(\tilde{t}_2 \rightarrow \tilde{t}_1 Z) = 52\%$		$\mathcal{B}(\tilde{t}_2 \rightarrow \tilde{t}_1 Z) = 56\%$
	$\mathcal{B}(\tilde{t}_2 \rightarrow \tilde{t}_1 h) = 39\%$		$\mathcal{B}(\tilde{t}_2 \rightarrow \tilde{t}_1 h) = 41\%$
	$\mathcal{B}(\tilde{t}_1 \rightarrow c \tilde{\chi}_1^0) = 82\%$		$\mathcal{B}(\tilde{t}_1 \rightarrow c \tilde{\chi}_1^0) = 90\%$

- (1) \tilde{t}_1 is the NLSP with a small Δm ,
- (2) the branching ratios $\mathcal{B}(\tilde{t}_2 \rightarrow \tilde{t}_1 Z)$ and/or $\mathcal{B}(\tilde{t}_2 \rightarrow \tilde{t}_1 h)$ are significant,

can be realized.

The most important input parameters of the phenomenological MSSM (pMSSM) which can be used to reproduce such a spectrum are shown in Table I.

Note that a low value of $\tan \beta$ and a high value of m_A are motivated from the consistency of the measured branching ratios of the rare B -meson decays $B_s \rightarrow \mu^+ \mu^-$ and $B_d \rightarrow X_s \gamma$ with their SM predictions. In fact, we have checked that for both the benchmark models shown in Table I, the SUSY predictions for the two branching ratios above are well inside the 2σ experimental limits [17–19]. The slepton masses are irrelevant for our discussion except the fact that the light sleptons can help ameliorate the discrepancy between the experimental measurement and the SM prediction of the anomalous magnetic moment of the muon [20,21]. The relic density of the LSP for both benchmark models is also less than the Planck upper limit mentioned in the introduction. We have used the software package SuperIso Relic [22] to calculate the B -decay branching ratios, anomalous magnetic moment of the muon, and the dark matter relic density.

Note that the main difference between the two models in Table I is in the masses of \tilde{t}_1 and $\tilde{\chi}_1^0$. As model 2 has higher values of these masses, the mass gap between \tilde{t}_2 and \tilde{t}_1 is smaller, which in turn makes both the \tilde{t}_1 and the Z or h less boosted.

III. COLLIDER STRATEGY

As we already mentioned in the introduction, the relevant processes of our interest are

TABLE II. Event summary after individual selection cuts both for the SUSY benchmark points and the SM backgrounds. See text for more details.

Process	Production cross section	Simulated events	No. of events after						Final cross section (fb)	S (100 fb ⁻¹)	
			S1	S2	S3	S4	S5	S6			
Signal											
Model 1	10 fb	[23]	10 ⁵	6012	4902	2736	2359	2143	1718	17.2 × 10 ⁻²	4.3
Model 2	10 fb	[23]	10 ⁵	6170	5319	2813	2421	2081	1853	18.5 × 10 ⁻²	4.6
Backgrounds											
$t\bar{t}$	833 pb	[24]	10 ⁸	221747	148580	142	41	26	11	9.1 × 10 ⁻²	
$t\bar{t}Z(1j)$	1.12 pb	[25]	226110	2484	1444	8	7	1	1	0.5 × 10 ⁻²	
$t\bar{t}W^\pm(1j)$	770 fb	[26]	276807	1365	787	5	3	3	2	0.5 × 10 ⁻²	
$t\bar{t}h(1j)$	700 fb	[27]	231064	1893	1027	2	2	2	2	0.6 × 10 ⁻²	
$t/\bar{t}W^\pm(1j)$	64 pb	[28]	6518431	7596	5801	13	9	3	3	2.9 × 10 ⁻²	
$P_1P_2P_3(1j)$ ($P_i \in WZh$)	500 fb	[29]	313350	1475	1093	10	5	4	2	0.3 × 10 ⁻²	
$P_1P_2 + 1j/2j$ ($P_i \in Zh$)	5.5 pb	[29]	738779	2927	2646	3	3	3	3	2.2 × 10 ⁻²	
Total background										16.1 × 10 ⁻²	

$$\begin{aligned}
pp &\rightarrow \tilde{t}_2 \tilde{t}_2^* \rightarrow \tilde{t}_1 \tilde{t}_1^* ZZ \rightarrow ZZ \tilde{\chi}_1^0 \tilde{\chi}_1^0 c \bar{c} \hookrightarrow ZZ + \cancel{p}_T + \text{soft jets} \\
pp &\rightarrow \tilde{t}_2 \tilde{t}_2^* \rightarrow \tilde{t}_1 \tilde{t}_1^* Zh \rightarrow Zh \tilde{\chi}_1^0 \tilde{\chi}_1^0 c \bar{c} \hookrightarrow Zh + \cancel{p}_T + \text{soft jets} \\
pp &\rightarrow \tilde{t}_2 \tilde{t}_2^* \rightarrow \tilde{t}_1 \tilde{t}_1^* hh \rightarrow hh \tilde{\chi}_1^0 \tilde{\chi}_1^0 c \bar{c} \hookrightarrow hh + \cancel{p}_T + \text{soft jets}.
\end{aligned}$$

There are several SM processes which can mimic our signal. They are all listed in Table II. Although two Z or Higgs bosons are absent in most of the backgrounds, in practice there is always a possibility of the W boson being mistagged as a Z or even a Higgs boson. This fraction might not be very large but considering the gigantic cross sections for some of the backgrounds compared to the signal, the final contribution might not be negligible. Thus, a detailed simulation of all the background processes is necessary to make reliable predictions, as we present in the next section.

As the mass gap between \tilde{t}_2 and \tilde{t}_1 is not so small in our case, both the decay products of \tilde{t}_2 , namely, \tilde{t}_1 and the Z or the h , are expected to be moderately boosted. We thus consider the fully hadronic decays of the Z or the h in order to be able to reconstruct them using the jet substructure technique. Here we adopt the method proposed by Butterworth, Davison, Rubin, and Salam (BDRS) [30] for tagging the hadronically decaying Z or the Higgs boson. We briefly describe below the exact procedure used in our analysis, along with our other selection criteria.

As the first step of this algorithm, we construct ‘‘fat jets’’ using the Cambridge-Aachen algorithm (CA algorithm) [31], as implemented in the Fastjet package [32,33] with an R parameter of 1.0. We demand that the fat jets satisfy $p_T > 200$ GeV and pseudorapidity $|\eta| < 3.0$. We then take a fat jet j and undo its last clustering step to get the two subjets j_1 and j_2 , with $m_{j_1} > m_{j_2}$ by convention. The two quantities $\mu = m_{j_1}/m_j$ and $y = \Delta R_{j_1, j_2}^2 \times \min(p_{Tj_1}^2, p_{Tj_2}^2)/m_j^2$, where $\Delta R_{j_1, j_2}$ is the distance between

j_1 and j_2 in the $\eta - \phi$ plane, are then computed. If there is significant mass drop, i.e., $\mu < \mu_c$, and the splitting of the fat jet j into j_1 and j_2 is fairly symmetric, i.e., $y > y_c$, then we continue; otherwise we redefine $j = j_1$ and perform the same set of steps as described above on j_1 . The parameters μ_c and y_c are tunable parameters of the algorithm and are set to 0.67 and 0.10, respectively, in our analysis. If the above two conditions $\mu < \mu_c$ and $y > y_c$ are satisfied, then the mother jet j is taken and its constituents are reclustered into CA jets with $R = R_{\text{filt}} = \min(\Delta R_{j_1, j_2}/2, 0.4)$, resulting in a number of jets $j_1^{\text{filt}}, j_2^{\text{filt}}, j_3^{\text{filt}}, \dots, j_n^{\text{filt}}$ ordered in descending p_T . The vector sum of the first three hardest jet momenta is then considered the Higgs candidate. The last step (the so called ‘‘filtering’’ procedure) is known to capture the dominant $\mathcal{O}(\alpha_s)$ radiation from the Higgs decay, while eliminating much of the contamination from underlying events [30].

Once the BDRS procedure is applied on the fat jets, we then impose the following selection criteria on the events:

- (i) S1: We demand that the two hardest fat jets (with $p_T > 200$ GeV, as mentioned before) reconstruct to either a Z or a Higgs boson with the mass windows [83.5–98.5] GeV and [118.5–133.5] GeV, respectively.
- (ii) S2: As our signal events have no top quark in them but most of the backgrounds do, we find it useful to veto events which have a top quark in them. In order to accomplish that, we again construct fat jets out of all the stable hadrons and apply the John Hopkins top tagger (JHToptagger) [34] on them. As the top quarks in the backgrounds are mostly not highly boosted, we use a comparatively large R parameter $R = 1.6$ in order to not lose most of the top quarks from the backgrounds. We set the other parameters of the JHToptagger algorithm [34] to be $\delta_p = 0.10$,

$\delta_r = 0.19$, $\cos \theta_h^{\max} = 0.7$, and the W mass window = (60–100) GeV. We demand that the final reconstructed top mass fall in the window (158.3–188.3) GeV. We do not demand any b tag for the reconstruction. An event is discarded if any of the fat jets reconstructs to a top quark by the above criteria.

As we do not also expect any hard leptons in the signal, we veto events which have any lepton with $p_T > 50$ GeV and $|\eta| < 2.5$. In addition to that, we also demand that the number of normal $R = 0.4$ anti- K_T jets [35] with $p_T > 50$ GeV and $|\eta| < 2.5$ be less than 6. Note that this step kills the multijet background configurations, e.g., $t\bar{t}$ + additional hard jets, while keeping almost all the signal events.

- (iii) S3: As \tilde{t}_2 is much heavier than both \tilde{t}_1 and the Z or h , the \tilde{t}_1 in the decay $\tilde{t}_2 \rightarrow \tilde{t}_1 h/Z$ is expected to be rather energetic, and a large part of its energy will be carried out by the LSP. Hence, even though Δm is rather small, the LSP will be quite energetic to record a high \cancel{p}_T in the detectors. A strong cut $\cancel{p}_T > 400$ GeV reduces the backgrounds by a huge amount while keeping a handful of signal events.
- (iv) S4: Since the charm jet from the decay of \tilde{t}_1 is very soft, the topology of the decay $\tilde{t}_2 \rightarrow \tilde{t}_1 (\rightarrow c\tilde{\chi}_1^0)Z/h$ looks exactly like the one where a mother particle decays to a visible daughter particle and an invisible particle. This observation motivates us to construct the transverse mass M_{T2} [36] out of the reconstructed Z and/or the h momenta and the missing transverse momentum. The M_{T2} constructed in this way should be distributed till the \tilde{t}_2 mass for the signal while the backgrounds are expected to populate the low mass region, because there is no such heavy mother particle for the backgrounds. Requiring a large value of M_{T2} , $M_{T2} > 400$ GeV, helps us to tame the backgrounds efficiently.
- (v) S5: The distribution of the effective mass of the system, $m_{\text{eff}} = \sum p_T(\text{hard jets and hard leptons}) + \cancel{p}_T$, being strongly correlated to $2m_{\tilde{t}_2}$ for the signal, is expected to occupy a much higher mass region compared to the background. In our analysis, we require $m_{\text{eff}} > 1250$ GeV to reduce the backgrounds further.
- (vi) S6: As the last step of our analysis, we demand that there be no more than two normal jets (anti- K_T , $R = 0.4$, $p_T > 50$ GeV, and $|\eta| < 2.5$ as in S2) with $\Delta R > 1.0$ with the two reconstructed Z 's or the h . We then also demand that none of these two jets be b -tagged. We use a 70% efficiency for b -tagging and the rate for a c jet (light jet) mistagged as a b jet to be 15% (1%) [37].

We use Pythia6.4.24 [38] for generating the signal events. For most of the the backgrounds, we use

Madgraph5 [29] to generate parton level events and subsequently use the Madgraph-Pythia6 interface (including matching of the matrix element hard partons and shower generated jets following the MLM prescription [39], as implemented in Madgraph5) to perform the showering and implement our event selection cuts.

IV. RESULTS AND DISCUSSION

In Table II we show the number of signal events for our two benchmark models, as well as all the backgrounds after each of the selection criteria described in the previous section has been used. In column 10 we show the final cross section when all the selection cuts have been imposed.

Note that the number of events simulated for all the backgrounds is more than the numbers of events expected at the 14 TeV LHC with 100 fb^{-1} integrated luminosity. Thus, our estimation of the backgrounds is expected to be quite robust. In the first column, the numbers within the brackets show the maximum number of additional jets which has been generated in Madgraph. For the $t\bar{t}$ background, we have generated a huge number (10^8) of events in Pythia6 (that means without additional hard jets) and checked that our background estimate agrees with a smaller sample of MLM matched $t\bar{t}$ + jets events generated in Madgraph. We have also checked that the contributions of the processes $t/\bar{t}Z$ + jets, $t/\bar{t}h$ + jets, W^+W^- + jets, $W^\pm Z$ + jets, and $W^\pm h$ + jets to the background are negligible.

In the ultimate column of Table II, we show the signal significance for an integrated luminosity of 100 fb^{-1} . While calculating the significance (S) we use the simple recipe of S/\sqrt{B} , S and B being the total number of signal and background events, respectively. Any additional systematic uncertainty (which is difficult to estimate in a phenomenological study) might change the significance somewhat but will not change the conclusion of our analysis in any significant way. It can be seen that a significance $S \sim 4\text{--}5$ can be obtained with approximately 100 fb^{-1} of data.

In conclusion, we have considered the possibility of detecting a SUSY signal for the light top squark NLSP scenario by considering the pair production of the heavier top squark instead of the commonly considered light top squark pair production channel. We have focused on the two decay channels $\tilde{t}_2 \rightarrow \tilde{t}_1 Z$ and $\tilde{t}_2 \rightarrow \tilde{t}_1 h$, giving rise to the spectacular diboson + missing transverse energy final state. Employing the jet substructure techniques to reconstruct the hadronically decaying Z and/or Higgs momenta, which also enables us to construct the M_{T2} out of the diboson momenta and the \cancel{p}_T , we have shown that a signal can be seen at the 14 TeV LHC with about 100 fb^{-1} integrated luminosity. It is worth mentioning at this point that there is a region of MSSM parameter space where the decay $\tilde{t}_2 \rightarrow \tilde{t}_1 h$ itself can also be substantial [14], and the possibility to see even just the di-Higgs signal should be investigated. This could also be important in the context of

Higgs self-coupling measurements which is extremely important in our endeavor to look for signatures of new physics beyond the SM.

ACKNOWLEDGMENTS

We thank JoAnne Hewett and Tom Rizzo for the hospitality at the SLAC Theory Group where this work was

started. We also thank Prateek Agrawal, Wolfgang Altmannshofer, Martin Bauer, Patrick Fox, Raoul Röntsch, and Felix Yu for useful discussions. The research leading to these results has received funding from the European Research Council under the European Union's Seventh Framework Programme (FP/2007-2013)/ERC Grant No. 279972.

-
- [1] S. P. Martin, [arXiv:hep-ph/9709356](#).
 - [2] C. Boehm, A. Djouadi, and M. Drees, *Phys. Rev. D* **62**, 035012 (2000).
 - [3] P. Ade *et al.* (Planck Collaboration), [arXiv:1303.5076](#).
 - [4] K.-i. Hikasa and M. Kobayashi, *Phys. Rev. D* **36**, 724 (1987).
 - [5] M. Muhlleitner and E. Popena, *J. High Energy Phys.* **04** (2011) 095.
 - [6] M. Carena, A. Freitas, and C. Wagner, *J. High Energy Phys.* **10** (2008) 109.
 - [7] B. He, T. Li, and Q. Shafi, *J. High Energy Phys.* **05** (2012) 148.
 - [8] M. Drees, M. Hanussek, and J. S. Kim, *Phys. Rev. D* **86**, 035024 (2012).
 - [9] D. S. Alves, M. R. Buckley, P. J. Fox, J. D. Lykken, and C.-T. Yu, *Phys. Rev. D* **87**, 035016 (2013).
 - [10] P. Agrawal and C. Frugiuele, [arXiv:1304.3068](#).
 - [11] G. Belanger, D. Ghosh, R. Godbole, M. Guchait, and D. Sengupta, [arXiv:1308.6484](#).
 - [12] CERN Report No. ATLAS-CONF-2013-068, 2013 (unpublished).
 - [13] D. Berenstein, T. Liu, and E. Perkins, *Phys. Rev. D* **87**, 115004 (2013).
 - [14] G. Belanger, F. Boudjema, and K. Sridhar, *Nucl. Phys.* **B568**, 3 (2000).
 - [15] A. Djouadi, J. Kneur, and G. Moultaka, *Nucl. Phys.* **B569**, 53 (2000).
 - [16] A. Djouadi, M. Muhlleitner, and M. Spira, *Acta Phys. Pol. B* **38**, 635 (2007).
 - [17] D. Asner *et al.* (Heavy Flavor Averaging Group), [arXiv:1010.1589](#).
 - [18] R. Aaij *et al.* (LHCb Collaboration), *Phys. Rev. Lett.* **111**, 101805 (2013).
 - [19] S. Chatrchyan *et al.* (CMS Collaboration), *Phys. Rev. Lett.* **111**, 101804 (2013).
 - [20] G. Bennett *et al.* (Muon G-2 Collaboration), *Phys. Rev. D* **73**, 072003 (2006).
 - [21] C. Gnendiger, D. Stöckinger, and H. Stöckinger-Kim, *Phys. Rev. D* **88**, 053005 (2013).
 - [22] A. Arbey and F. Mahmoudi, *Comput. Phys. Commun.* **181**, 1277 (2010).
 - [23] W. Beenakker, R. Hopker, and M. Spira, [arXiv:hep-ph/9611232](#).
 - [24] M. Aliev, H. Lacker, U. Langenfeld, S. Moch, P. Uwer, and M. Wiedermann, *Comput. Phys. Commun.* **182**, 1034 (2011).
 - [25] A. Kardos, Z. Trocsanyi, and C. Papadopoulos, *Phys. Rev. D* **85**, 054015 (2012).
 - [26] J. M. Campbell and R. K. Ellis, *J. High Energy Phys.* **07** (2012) 052.
 - [27] S. Dawson, C. Jackson, L. Orr, L. Reina, and D. Wackerroth, *Phys. Rev. D* **68**, 034022 (2003).
 - [28] J. M. Campbell and F. Tramontano, *Nucl. Phys.* **B726**, 109 (2005).
 - [29] J. Alwall, M. Herquet, F. Maltoni, O. Mattelaer, and T. Stelzer, *J. High Energy Phys.* **06** (2011) 128.
 - [30] J. M. Butterworth, A. R. Davison, M. Rubin, and G. P. Salam, *Phys. Rev. Lett.* **100**, 242001 (2008).
 - [31] Y. L. Dokshitzer, G. Leder, S. Moretti, and B. Webber, *J. High Energy Phys.* **08** (1997) 001.
 - [32] M. Cacciari and G. P. Salam, *Phys. Lett. B* **641**, 57 (2006).
 - [33] M. Cacciari, G. P. Salam, and G. Soyez, *Eur. Phys. J. C* **72**, 1896 (2012).
 - [34] D. E. Kaplan, K. Rehermann, M. D. Schwartz, and B. Tweedie, *Phys. Rev. Lett.* **101**, 142001 (2008).
 - [35] M. Cacciari, G. P. Salam, and G. Soyez, *J. High Energy Phys.* **04** (2008) 063.
 - [36] C. Lester and D. Summers, *Phys. Lett. B* **463**, 99 (1999).
 - [37] CERN Report No. CMS-PAS-BTV-09-001, 2009 (unpublished).
 - [38] T. Sjostrand, S. Mrenna, and P. Z. Skands, *J. High Energy Phys.* **05** (2006) 026.
 - [39] S. Hoeche *et al.*, [arXiv:hep-ph/0602031](#).